light region.

(2) Field induced strain

It was first observed by the real time study that the specimen plate was bent when the electric field was applied normal to the specimen surface. The crystal became concave always towards negative potential side of the electrodes. This effect was temperature dependent and was very marked near the phase transition point T_C=120° C. The curvature of the specimen was measured in the temperature range 25-150°C and the field strength up to 10kV/cm. This effect is explained by the electrostrictive effect and inhomogeneous distribution of the electric field in $BaTiO_3$ crystal (H.Motegi; J.Phys.Soc.Jpn. 32(1972)202). The speed of the response of this field induced lattice strain to increasing and decreasing fields were different.

(3) Phase transition

The ferroelectric-paraelectric phase transition at T_C was observed. The movement of the phase boundaries and the ferroelectric domain formation have clearly been observed in real time.

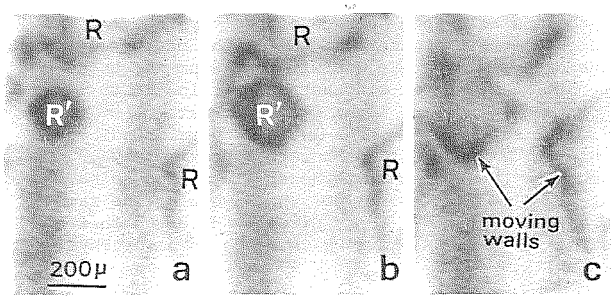

Fig.1 Domain switching in $BaTiO_3$. Mo-Ka(200).

11.1-11 ON THE CONTRAST OF DISLOCATIONS IN X-RAY SECTION TOPOGRAPHY. By J. Gronkowski and G. Kowalski, Institute of Experimental Physics, University of Warsaw, Warsaw, Poland.

The contrast of a 60° dislocation in a Si single crystal is studied by X-ray section topography ($MoK_{\alpha 1}$ radiation, $(2\bar{2}0)$ reflection, μt=0.6). Numerical simulations of the images in dependence on the dislocation position in the Borrmann fan (Fig. 1) are compared with their experimental counterparts (Fig. 2, courtesy of Dr. Lefeld-Sosnowska, from Phys. Stat. Sol. (a) (1978) 48, 565). It was found that for strong contrast conditions the intermediary image (Authier, Adv. X-Ray Anal. (1967) 10, 9) may be interpreted as well-known Kato fringes for a wedge crystal (Kato, Lang, Acta Cryst. (1959) 12, 787). The direct image depends strongly on the position of the dislocation line and arises not only when it is in the region near to the primary beam. The contrast itself depends only very weakly on the direction of the Burger's vector.

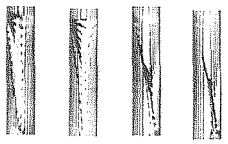

Fig. 1

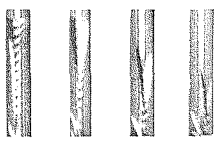

Fig. 2

11.1-12 STUDY OF ANTIPHASE DOMAIN BOUNDARIES BY X-RAY TOPOGRAPHY. By B.Capelle and C.Malgrange. Laboratoire Minéralogie et Cristallographie, Université Pierre et Marie Curie, Paris, France.

$GdDy(MoO_4)_3$ crystals are ferroelectric and ferroelastic below T_C = 159°C. The structure which is tetragonal ($P\bar{4}2_1m$) above T_C^c becomes orthorhombic (Pba2) below T_C, with a doubling of the unit cell and a rotation of 45° of the crystallographic axes. Consequently, in each ferroelectric domain, there can exist two antiphase domains which can be deduced from each other by a translation vector $\vec{f} = 1/2(\vec{a}+\vec{b})$. The structure factors of both domains are then respectively F_h and $F_h e^{i\phi}$, where $\phi = 2\pi \vec{h}.\vec{f}$. When ϕ is not a multiple of 2π, APB'S appear as plane defects for X-Rays. This occurs only in the case of superstructure reflections i.e. reflections which are forbidden in the high temperature phase. Now, since antiphase domain boundaries (APB'S) are observed not only in the case of superstructure reflections but also in that of "ordinary" reflections an additional translation vector $\Delta\vec{f}$ needs to be introduced.

From the contrast on various traverse topographs it is deduced that $\Delta\vec{f}$ is parallel to $\vec{a}$. In order to determine the value of $\Delta\vec{f}$, it is necessary :

- to determine the APB'S geometry
- to make section topographs
- to compare them with computer simulations

Two types of APB'S have been studied corresponding respectively to Laue-Laue case and Laue-Bragg case. In the first case, calculations were made on the basis of stationnary phase method ; in the second case, Takagi's equations were used.

The comparison between section topographs and simulations leads to a value of $\Delta\vec{f}$ of the order of a/30 corresponding to an expansion of the lattice inside the boundary.

LAUE-LAUE case
$\vec{h}(600)$

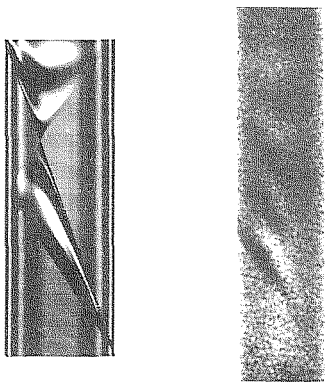

Fig. 1

LAUE-BRAGG case
$\vec{h}(600)$

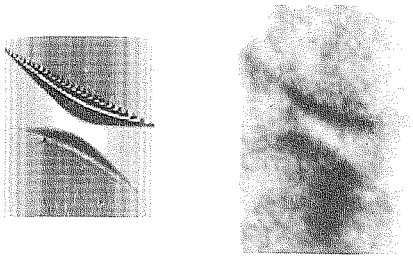

Fig. 2